

# A unified cross-attention model for predicting antigen binding specificity to both HLA and TCR molecules

Chenpeng Yu<sup>1</sup>, Xing Fang<sup>1</sup>, Hui Liu<sup>1\*</sup>

<sup>1</sup>College of Computer and Information Engineering, Nanjing Tech University, Nanjing, 211800, Jiangsu, China.

\*Corresponding author(s). E-mail(s): [hliu@njtech.edu.cn](mailto:hliu@njtech.edu.cn);

## Abstract

The immune checkpoint inhibitors have demonstrated promising clinical efficacy across various tumor types, yet the percentage of patients who benefit from them remains low. The binding affinity between antigens and HLA-I/TCR molecules plays a critical role in antigen presentation and T-cell activation. Some computational methods have been developed to predict antigen-HLA or antigen-TCR binding specificity, but they focus solely on one task at a time. In this paper, we propose UnifyImmun, a unified cross-attention transformer model designed to simultaneously predicts the binding of antigens to both HLA and TCR molecules, thereby providing more comprehensive evaluation of antigen immunogenicity. We devise a two-phase progressive training strategy that enables these two tasks to mutually reinforce each other, by compelling the encoders to extract more expressive features. To further enhance the model generalizability, we incorporate virtual adversarial training. Compared to over ten existing methods for predicting antigen-HLA and antigen-TCR binding, our method demonstrates better performance in both tasks. Notably, on a large-scale COVID-19 antigen-TCR binding test set, our method improves performance by at least 9% compared to the current state-of-the-art methods. The validation experiments on three clinical cohorts confirm that our approach effectively predicts immunotherapy response and clinical outcomes. Furthermore, the cross-attention scores reveal the amino acids sites critical for antigen binding to receptors. In essence, our approach marks a significant step towards comprehensive evaluation of antigen immunogenicity.

**Keywords:** Cross-attention mechanism, neoantigen, T-cell receptor, Human leukocyte antigen, Virtual adversarial training, Integrated gradient

# 1 Introduction

The anticancer immune response involves a sequence of intricate biological events that lead to effective kill of cancer cells. Initially, tumor antigens are released by cancer cells through specific mechanism, and are captured and processed by antigen-presenting cells (APCs) [1]. These APCs present the antigens on their outer surface (antigen presentation). When naive T cells recognize and bind to the presented antigens, they become activated (T-cell activation) and subsequently differentiate into effector T-cells, such as cytotoxic T lymphocytes (CTLs) [2][3][4][5][6]. The effector T-cells migrate to the tumor site and attack cancer cells [7], ultimately inducing their death [8]. Additionally, some T-cells differentiate into memory T-cells, which persist in the body for extended periods and provide long-term immunological memory [9][10]. These steps are referred to as Cancer-Immunity Cycle [11], which indeed highlight a delicate balance between the recognition of non-self antigens and the prevention of autoimmunity. Within this cycle, antigen presentation and T cell activation stand out as two steps critical to the success of the anticancer immune response [12][13].

The binding of peptides to class I human leukocyte antigen (HLA) molecules is a fundamental process in tumor antigen presentation [12]. HLA alleles are known for their high specificity and polymorphism in the human population [14], allowing them to selectively bind to a narrow range of peptides, thereby forming the peptide-HLA complex (pHLA) [15]. Identifying the peptides that are chosen for binding by specific HLA alleles is a critical step in epitope selection. Subsequently, the recognition of the presented antigens by T-cell receptors (TCR) is the prerequisite to activate T cells and trigger a robust immune response [15]. This process is also highly selective, and only a small subset of peptides can be recognized by TCRs. This selectivity, known as TCR binding specificity, arise from the high diversity of TCR repertoire (estimated to range from  $10^{15}$  to  $10^{61}$  possible receptors in humans) [16]. This diversity is primarily manifested in complementarity determining region 3 (CDR3) [17], which directly interacts with pHLA complex and determines the TCR binding specificity [18][19]. These binding specificity ensures that only relevant antigens are presented and activate immune system, maintaining the delicate balance between effective immune responses and autoimmune reactions.

The HLA polymorphism and TCR repertoire diversity represent evolutionary traits that enable the human immune system to respond to a wide array of pathogens at individual level [20][21]. Some experimental assays like mass spectrometry (MS)-eluted HLA ligands [22] and techniques such as single-cell TCR sequencing [23] and T-scan [24] have been developed to detect antigen-HLA and antigen-TCR bindings, respectively. However, these experimental assays are often time-consuming, technically complex, and costly. To address these challenges, some computational methods have emerged as viable alternatives for predicting peptide binders [25]. These methods include TransPHLA[26], MHCflurry[27], netMHCpan4.0[28], DeepLigand[29], BERTMHC[30] for peptide-MHC binding prediction, as well as PanPep[31], pMTnet[32], DLpTCR[33], ERGO2[34], TITAN[35] and ATMTTCR [36] for peptide-TCR binding prediction. Although some methods have achieved impressive prediction accuracy, they all consider the antigen-HLA and antigen-TCR binding prediction as separate tasks. Existing methods overlook a crucial

fact: the immunogenicity of antigens is profoundly influenced by their binding affinity to both HLA and TCR molecules, rather than solely relying on one type of binding.

Distinct from previous studies that considered HLA or TCR binding specificity alone, we propose a unified model UnifyImmun, which integrates the predictive tasks of HLA-antigen and TCR-antigen binding to establish a one-stop deep learning framework for comprehensive evaluation of antigen immunogenicity. As shown in Figure 1, UnifyImmun comprises three self-attention-based encoders that receive HLA, antigen, and TCR sequences as inputs, respectively. While these encoders share a common network structure, they operate with distinct parameters. They independently map the input sequences into embedding vectors in latent space. Subsequently, to effectively fuse the information of peptides and receptors, two cross-attention modules are employed. These modules receive as inputs the latent representations of HLA-antigen and TCR-antigen pairs, respectively. The outputs of cross-attention modules are then passed through fully-connected layers and softmax transformations to generate predictions for HLA-antigen and TCR-antigen binding, respectively. Once training finished, our model can be independently applied to three prediction tasks: HLA-antigen binding, or TCR-antigen binding, or the binding of HLA- antigen-TCR. In particular, the cross-attention mechanism is instrumental in integrating receptor-ligand information, thereby facilitating the capture of critical information for antigen binding to HLA or TCR. Additionally, attention scores generated by our model offer valuable insights into the key positions and amino acids within the antigen sequence that are pivotal for effective antigen presentation and subsequent T cell activation. This aspect of our model contributes significantly to its interpretability, enhancing our understanding of the underlying immunological processes.

Given the vast diversity of HLA and TCR repertoires, the sequences currently available for model training are limited and even biased, posing a significant challenge of overfitting in the development of prediction models. To overcome this limitation, we introduced virtual adversarial training as a means to enhance the model generalizability. Specifically, we apply adversarial perturbations to the embeddings generated by three sequence encoders, generating virtual samples that aim to maximize the loss function. By enforcing the model to resist the adversarial perturbations, thereby its generalizability can be significantly improved. This adversarial training approach has demonstrated effective enhancement of the model performance (see Section 4.8).

Ideally, our model prefers to be trained using HLA-antigen-TCR triplet samples. However, the availability of such triplets is currently limited, whereas HLA-antigen and TCR-antigen binding data are relatively abundant. To efficiently leverage this available data, we propose a two-stage progressive training strategy (see Method for details). Through performance evaluation on multiple test datasets, we have demonstrated that the two-stage progressive training effectively enhances the feature extraction capabilities of the encoders, thereby improving the predictive performance of HLA-antigen and TCR-antigen binding specificity.

Our work achieves a significant advancement in the field, offering at least three notable contributions compared to previous studies:

- By integrating both prediction tasks within a unified model, our approach enables simultaneous evaluation of antigen presentation efficiency and T-cell activation

potential. This comprehensive assessment provides a more holistic view of antigen immunogenicity, offering deeper insights into the overall quality and potential efficacy of antigens in triggering immune responses.

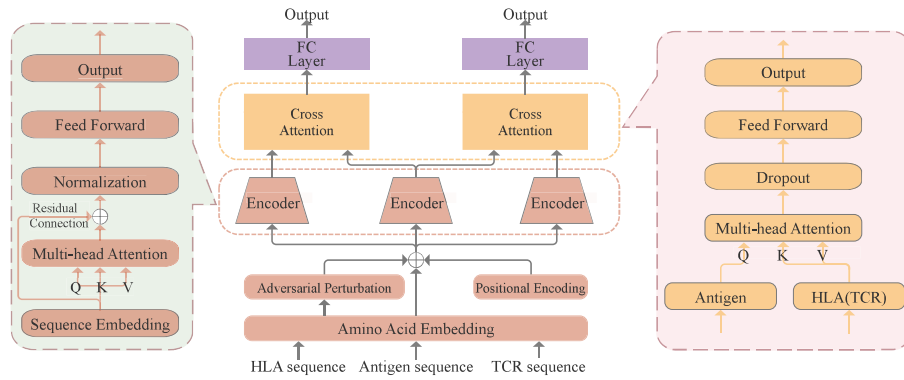
- We employ a unique antigen encoder to derive representations from antigen sequences, which are then utilized for both HLA-antigen and TCR-antigen binding predictions. This multitask learning stands in contrast to previous models that focused exclusively on either one alone. By sharing antigen presentation across tasks, our model significantly enhances generalization capabilities by leveraging commonalities in the underlying biology processes of antigen recognition.
- Our unified framework not only achieves superior performance for HLA-antigen binding predictions, but also boosts the predictive accuracy of TCR-antigen binding specificity. This multifaceted performance enhancement represents a substantial advantage over previous methodologies, highlighting the superiority of our approach in capturing the intricate relationships between HLA, TCR, and antigen sequences.

## 2 Results

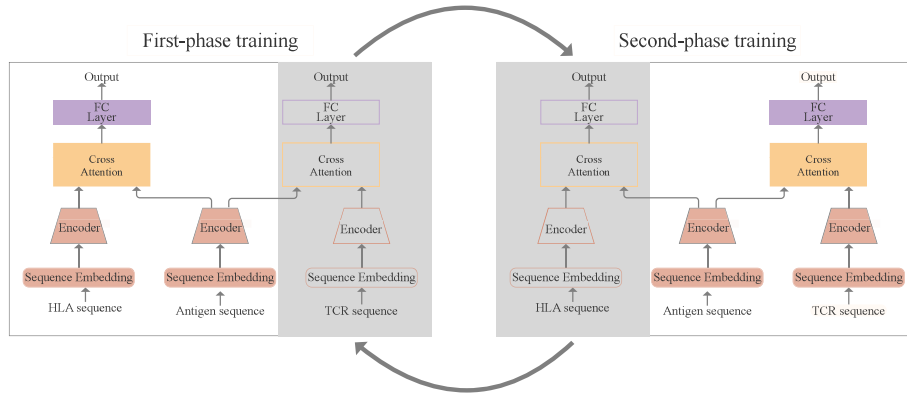
### 2.1 Performance evaluation on HLA-antigen binding prediction

To evaluate the proposed model’s predictive performance in HLA-antigen binding, we conducted performance comparison on a hold-out independent test, an external test, HPV and neoantigen validation datasets. We compared UnifyImmun against twelve established methods, including TransPHLA [26], NetMHCpan\_EL [28], NetMHCpan\_BA [28], ANN [37], PickPocket [38], SMMPMBEC [39], SMM [40], NetMHCcons [41], NetMHCstabpan [42] and Consensus [43], and two attention-based methods [26] published recently (ACME [44] and DeepAttentionPan [45]). which can be obtained from <http://tools.iedb.org/main/tools-api/>. These comparative methods were downloaded as executable packages from the IEDB database [46], and run on the same test sets using their default parameters. The performance metrics including AUROC, accuracy, MCC, and F1-score. Additionally, we provided additional metrics in the supplementary file, including precision, recall, AUPR, and specificity, to offer a more comprehensive evaluation of the model’s performance.

We firstly evaluated the performance of UnifyImmun against other comparative algorithms on a 10% hold-out test set. As shown in Figure 2(a), UnifyImmun remarkably outperformed all other methods across all evaluation metrics. In particular, compared to the second-best method, TransPHLA, UnifyImmun achieved at least a 5% improvement in both AUROC and AUPR. To provide a visual representation of the performance differences, Figure 2(b) presented the ROC curves and precision-recall curves for all comparative methods on the hold-out test set. These curves further validated the superior performance of our proposed method. Figure 2(c) visualized the UMAP feature of peptide-HLA pairs, implying the positive and negative samples separated remarkably in the latent space. To further assess the model’s ability to prioritize HLA-antigen pairs, we presented the positive predictive value (PPV) for the top 100, top 1000, and top 5000 predicted positive samples. As illustrated in Figure 2(d), UnifyImmun achieved an impressive 100% PPV for the top 100 predictions and maintained



(b) Two-phase progressive training



(c) Antigen sequence frequency

(d) CDR3 sequence frequency

**Fig. 1:** Illustrative diagram of UnifyImmun framework and two-phase training strategy, as well as frequency distribution w.r.t sequence lengths. (a) Architecture of UnifyImmun based on cross-attention mechanism. (b-c) Frequency of antigen sequences and TCR CDR3 sequences included in positive training samples with respect to lengths.

excellent performance above 97% for both the top 1000 and top 5000 predictions. In contrast, the other methods did not demonstrate comparable ability in prioritizing HLA-antigen pairs.

For objective performance evaluation, we conducted tests on an external dataset provided by TransPHLA. As shown in Figure 2(b), while TransPHLA exhibited performance advantages on its own dataset, UnifyImmun achieves nearly identical performance to TransPHLA. Furthermore, UnifyImmun notably outperformed all other methods across all performance metrics, except for TransPHLA.

The HPV antigens came from a previous study [47] that identified 278 experimentally verified pHLA bindings derived from the HPV16 proteins E6 and E7, consisting of peptides ranging from 8 to 11 amino acids in length [48] [49]. UnifyImmun achieved an impressive accuracy rate of 83.8%. This significantly surpassed the performance of the current state-of-the-art model TransPHLA, which exhibited a screening rate of only 68%. For neoantigen validation, we used the dataset released by TransPHLA. These neoantigens were collected from non-small-cell lung cancer, melanoma, ovarian cancer and pancreatic cancer in recent studies. This dataset includes 221 experimentally verified pHLA bindings. UnifyImmun achieved 94.1% accuracy (208 out of 221), which is comparable to TransPHLA with 96.4%. Collectively, the performance comparison experiments on four distinct datasets clearly demonstrated the superior generalization capability of UnifyImmun compared to the current state-of-the-art methods.

## 2.2 UnifyImmun boosts the predictive performance of TCR-antigen binding specificity

Our model can actually predict TCR-antigen binding specificity. To assess its performance, we conducted a comparative analysis with four current state-of-the-art methods in the field, including Pan-Peptide, ERGO2, pMTnet and DLpTCR. For a fair assessment, we executed the executable codes of Pan-Peptide, ERGO2, and pMTnet using recommended parameters on the same workstation as UnifyImmun. For DLpTCR, we accessed its web server for evaluation. We initially evaluated the performance of all methods on a 10% hold-out test set. As shown in Figure 3(a), UnifyImmun remarkably outperformed all other methods on this hold-out test set. Specifically, UnifyImmun achieved AUROC and AUPR values of 0.938 and 0.936, respectively, highlighting its exceptional predictive ability in TCR-antigen binding specificity. Among the comparative methods, only ERGO2 exhibited moderate performance, with AUROC and AUPR values of 0.704 and 0.747, respectively. The remaining methods, Pan-Peptide, pMTnet, and DLpTCR, performed close to random guessing, indicating significant limitations in their predictive capacity for TCR-antigen binding specificity.

To further validate the performance of UnifyImmun objectively, we compiled an external independent test set consisting of over 100,000 TCR-pHLA binding pairs collected from a number of publications. This comprehensive dataset allowed us to assess the predictive capabilities of UnifyImmun toward real-world scenario, beyond the initial hold-out test set. The experimental results were consistent with our previous findings, further confirming the superior performance of UnifyImmun. As shown in Figure 3(b), UnifyImmun achieved AUROC and AUPR values exceeding 0.9,

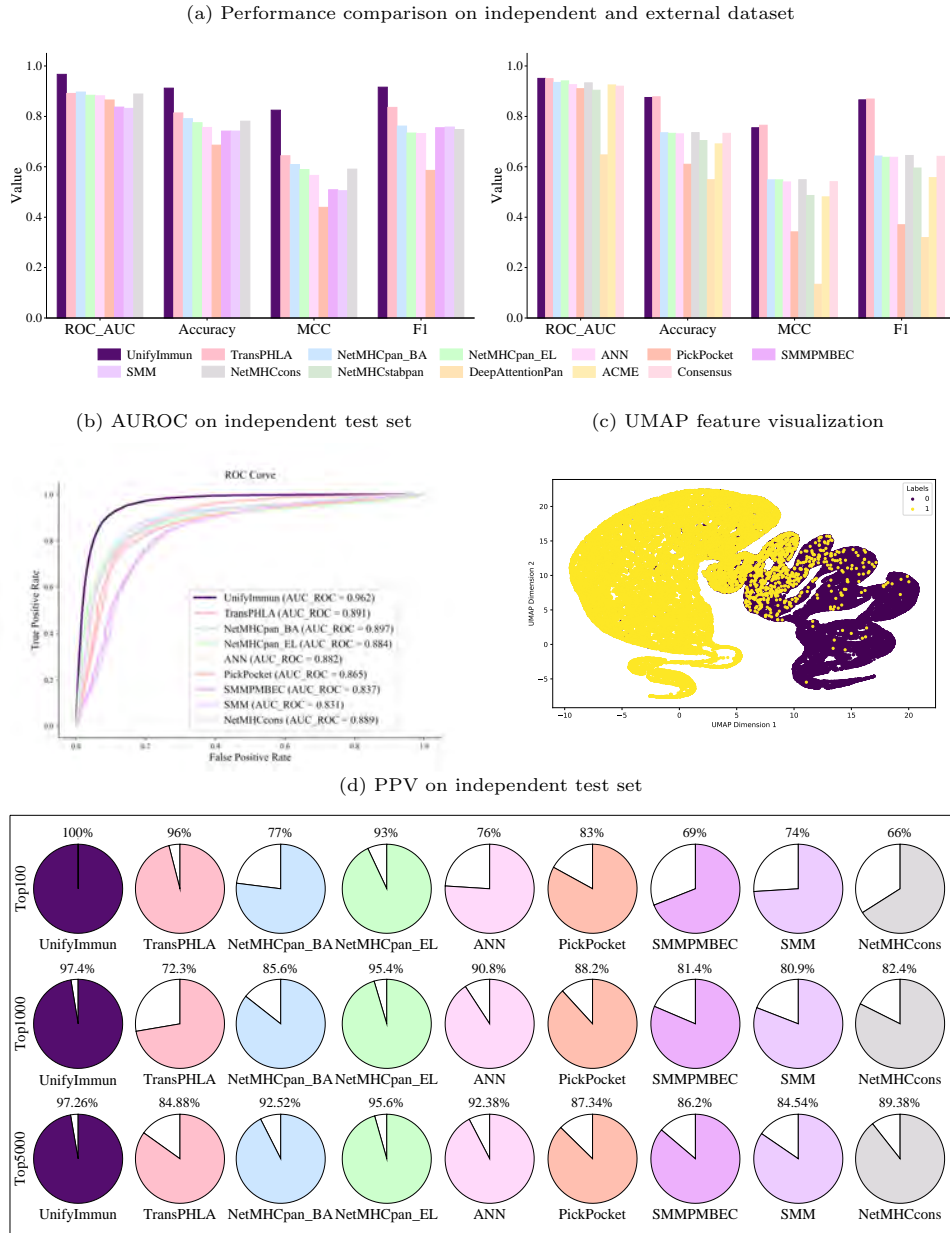


**Fig. 2:** Performance evaluation on predicting peptide-HLA binding specificity. (a) Performance comparison to twelve existing methods on independent and external test dataset, respectively. (b) ROC curves and AUC values achieved by UnifyImmun and eight comparative methods on independent test set. (c) UMAP feature visualization of peptide-HLA pairs. (d) Positive predictive value (PPV) for the top 100, top 1000, and top 5000 predicted positive samples.

significantly outperforming the second-best method, ERGO2. The other three methods—PanPep, pMTnet, and DLpTCR—exhibited even poorer performance. We even observed negative MCC values for PanPep and DLpTCR, indicating a high degree of disagreement between the model predictions and the actual outcomes. This observation further underscores the limitations of these comparative methods, which in turn validated the superior performance of UnifyImmun in predicting TCR-antigen binding specificity.

Moreover, we computed the positive predictive value (PPV) for the top-ranked predicted positive TCR-antigen samples on two distinct datasets. Specifically, we evaluated the PPV for the top 100, top 1000, and top 5000 predictions (Figure 3(c-d)). UnifyImmun achieved an impressive 100%, 99% and 97% PPV values for the top 100, top 1000 and top 5000 predictions, respectively. In contrast, the other methods performed significantly worse in this aspect. Additionally, we also presented the ROC curves and AUC values for these methods on both test sets (Figures 3(e-f)). The UMAP feature visualization of peptide-HLA pairs implied that the positive and negative samples separated remarkably in the latent space (Figure 2(g-h)). It can be found that UnifyImmun exhibited superior performance in predicting TCR-antigen binding specificity compared to the other methods. It is indeed noteworthy that while the comparative methods may exhibit better performance on smaller datasets, their performance decreased seriously when applied to large-scale test set. This suggests they suffered from weak generalization ability and struggle to adapt to large real-world data scenarios. In contrast, UnifyImmun demonstrated strong robustness across distinct datasets, offering a more dependable and precise tool for predicting TCR-antigen binding specificity.

### 2.3 Two-phase progressive training effectively improve model performance

Due to the limited number of HLA-antigen-TCR triplet samples for model training, we devised a two-phase progressive training strategy aimed at effectively leveraging the HLA-antigen and TCR-antigen binding samples available. To validate the performance enhancement by two-stage progressive training strategy, we randomly divided the benchmark dataset into training and test sets for model training and subsequent assessment. This process was independently repeated ten times to account for variations introduced by random data partitioning. Next, We presented the results in boxplots for each training round. This approach allows us to confidently evaluate the effectiveness of our methodology while mitigating any potential biases introduced by random data partition.

As depicted in Figures 4, the model performance was suboptimal in the absence of alternating training (Round 0). However, as the number of training rounds increased, we observed a marked and consistent improvement in model performance until it converged at a high level. Specifically, on the HLA-antigen hold-out test set, the two-phase alternative training quickly boosted both AUROC and AUPR values (Figures 4(a-b)). For TCR-antigen binding prediction, similar trends were observed on both hold-out and external test datasets (Figures 4(c-f)). To further validate the effectiveness of our training strategy, we evaluated the model’s predictive power on a COVID-19 test set



(for data detail see Section 2.5). As expected, the results showed that the performance on the COVID-19 test set improved with an increasing number of training rounds (Figures 4(g-h)). Notably, while the variance in performance metrics was higher in the early rounds, it decreased progressively as the number of alternating rounds increased. This indicates that the model’s performance became less affected by random data partitioning. These findings confirm that the two-stage progressive training strategy drives the model to learn more effective feature representations, thereby achieving more stable and reliable performance.

## 2.4 Cross-attentions and integrated gradients reveal important locus

We employed a cross-attention mechanism to integrate information from antigens with HLA/TCR, aiming to explore whether cross-attention scores reflect the crucial positions and amino acids in the antigen sequence for its binding affinity to HLA and TCR receptors. For this purpose, we aggregated the attention scores for each amino acid at every position across all antigen sequences. Higher scores indicate strong influence on the binding affinity to the receptors. To accommodate variations in antigen length, we generated separate heatmaps based on the cross-attention scores for antigens of lengths 9-14 (Figure 5(a-b) and Figure S3).

For binding to HLA, the attention scores are significantly higher at the second and final position of the antigen sequence, indicating that these two loci are particularly important for strong binding affinity. Notably, the Leu amino acid (L) consistently receives higher attention scores, especially at these critical positions, emphasizing its significance in antigen-HLA interactions. When considering TCR-antigen binding, we also found that the Leu amino acid at the second position [50] stands out as the most influential. To gain a more comprehensive understanding of the amino acids contributions, we calculated the cumulative attention scores for each amino acid across all positions in antigens of specific lengths. This metric reflects the overall importance of an amino acid in mediating antigen-receptor binding. Figures 5(e-f) graphically illustrated the attention scores for all 20 amino acids in the context of HLA and TCR binding, respectively. It is evident that Leu consistently plays a pivotal role in antigen binding to both receptors, regardless of antigen length.

To further validate the findings from cross-attention heatmaps, we calculated the Integrated Gradients (IG) values for each amino acid at every position within the antigen sequences. As shown in Figure 5(e-f), there were strong correlations between the IG values and the attention score heatmaps. For instance, the Leu amino acid at the second position within the antigen sequence emerged as particularly important for the binding affinity to both HLA and TCR molecules. The consistency between the attention scores and the IG values reinforced the validity of our approach and highlights the crucial role of specific amino acids and their positions in mediating antigen-receptor affinity.

To intuitively illustrate the crucial positions and amino acids involved in TCR-pHLA binding, we obtained the crystal structure of the TK3 TCR in complex with HLA-B\*3501/HPVG (PDB ID: 3MV7) from the PDB database. We extracted the

HLA allele, antigen (11-mer), and the CDR3 $\beta$  chain (11-mer) and predicted their binding scores using UnifyImmun. The results indicated a high binding score between HLA and antigen (0.99), as well as a moderate score between the CDR3 $\beta$  chain and antigen (0.62). Upon careful inspection of the three-dimensional structure (Figure 5(g)), we observed that the 9-th amino acid Phe (Y) of the antigen is embedded within the HLA binding groove (represented by blue helices) and stabilized through hydrogen bonds (yellow lines). This observation illustrated the chemical mechanism underlying the binding of the antigen to HLA. Furthermore, the attention heatmap for the HLA-antigen-TCR ternary complex (Figure 5(h)) revealed a significant cross-attention score between the 8-th amino acid Tyr (Y) of the antigen and the 8-th amino acid Gly (G) on the CDR3 $\beta$  chain. The crystal structure demonstrated the formation of hydrogen bonds associated with these two amino acids, indicating their crucial role in the formation of the pTCR complex, despite their distance of 8.77Å (distance between two C $\alpha$  atoms of two amino acids) is slightly beyond the conventional contact threshold of 6Å. In summary, the cross-attention mechanism offers opportunity to explore the global dependencies between TCR-pHLA interactions, thereby enhancing the interpretability of our model.

## 2.5 UnifyImmun generalizes to COVID-19 antigen-TCR binding specificity

To validate the generalizability of UnifyImmun, we tested its ability to predict the bindings between virus-derived antigens and TCRs. We collected a total of 520,000 positive interactions between antigens derived from COVID-19 virus and human TCRs from the ImmuneCODETM database. Meanwhile, we generated an equal number of negative samples via random shuffle, creating a million-scale COVID-19 test set. We compared UnifyImmun with several other methods, including PanPen, ERGO2, DLpTCR, and pMTnet. Due to the low efficiency of pMTnet and DLpTCR, they were unable to tackle million-scale test set within a reasonable time frame. Therefore, we randomly selected 100,000 pair as their test set for evaluation.

The results showed that UnifyImmun achieved AUROC and AUPR values of 0.644 and 0.632, respectively (Figure 6(a)). In contrast, other methods obtained AUROC and AUPR values only marginally above 0.5, which is close to random guessing. Furthermore, we computed the PPV values for the top 100, top 1000, and top 5000 predictions made by each method. Our model consistently achieved 90% PPV values, remarkably outperformed all the comparative methods whose PPV values were always less than 60%. Overall, this significant difference provide strong evidence of the robust generalizability of UnifyImmun. Its ability to accurately predict antigen-TCR bindings, even for external virus-derived antigens, highlights its potential for facilitating the development of effective immune-based therapies and vaccines against COVID-19 viruses, including .

## 2.6 Validation of UnifyImmun predictive power on immunotherapy responses and clinical outcomes

The antigen presentation to cytotoxic T-cells plays a pivotal role in determining the efficacy of tumor immunotherapy, particularly with immune checkpoint inhibitors. To evaluate the predictive power of UnifyImmun, we conducted a comprehensive study on a metastatic melanoma cohort (MM-HLA) [51] and a urothelial carcinoma cohort (UC) [52]. The MM-HLA cohort included 110 patients, with each individual harboring an average of 919 potential neoantigens. The UC cohort included 18 patients, with each patient harboring 115 potential neoantigens. For each patient, we obtained the HLA typing, tumor antigen sequences, and the clinical immunotherapy responses. For the MM-HLA cohort, we utilized the RECIST criteria to categorize patients into four distinct groups: complete response (CR), partial response (PR), stable disease (SD), and progressive disease (PD). We predicted the binding scores for all possible HLA-peptide pairs using UnifyImmun and visually represented the predicted scores for each patient group. As shown in Figure 7(a), analysis of variance (ANOVA) with an  $F$ -test revealed statistically significant differences in the HLA-peptide binding affinity between these groups. Notably, the PD group demonstrated a highly statistical divergence compared to the other patient groups (CR, PR and SD). This observation underscored the distinct differences in neoantigen presentation between benefit vs non-benefit patient groups from immunotherapy. Moreover, the patients in the CR group exhibited the prevalence of high-affinity neoantigens, while those in the PD group showed many low-affinity antigens. Furthermore, we stratified the patients based on response, non-response, and long survival (PFS<180 days but OS>2 years), and the violin plots further confirmed that the three groups exhibited distinct patterns in antigen binding affinity to HLA molecules (Figure 7(b)). In the UC cohort, the CR group also exhibited a notable presence of high-affinity antigens (Figure 7(c)), and ANOVA analysis further showed noteworthy differences between these groups. Notably, while the differences between the PR and SD groups were not as pronounced, the PD group exhibited the highly significant divergence from the others. Figure 7(d) visualized the distinct patterns of antigen presentation between the clinical response and non-response groups. The findings supported the clinical utility of UnifyImmun in guiding treatment decisions and ultimately improving patient outcomes.

To further validate the predicted antigen-TCR pairs, we conducted analysis on additional advanced melanoma cohort (MM-TCR) that had received immunotherapy [53]. This cohort comprised 29 patients who underwent TCR-seq and genomic sequencing. Using the amino acid resulting from a missense mutation as an anchor, we generated all possible 9-mer peptides harboring this anchor site. After extracting the CDR3 sequences from TCR-seq data, we created all possible CDR3-peptide pairs for each patient, yielding a total of 81,851,486 pairs. We used UnifyImmun to score these CDR3-peptide pairs, and selected the top 5000 highest-scoring peptide-TCR pairs for each patient. Next, we categorized the patients into CR, PR, SD, and PD groups based on RECIST criteria, and plotted the boxplots of the predicted scores for each group (Figure 7(e)). ANOVA analysis revealed significant differences among the groups ( $F$ -test), with the CR and PR groups exhibiting notably higher scores than the SD and

PD groups. By stratifying the patients into benefit, non-benefit, and long-term survival groups, we generated the violin plots (Figure 7(f)) and found that patients in the long-term survival group exhibited peptide-TCR pairs with higher binding scores.

Finally, to confirm the correlation between high-confidence HLA- and TCR-peptide pairs by UnifyImmun and improved clinical outcomes, we conducted survival analysis on two melanoma cohorts (MM-HLA and MM-TCR). We considered the top 2% HLA- and TCR-peptide pairs as high-confidence bindings, and stratified the patients with such bindings into the high-confidence group, while the remaining patients into the low-confidence group. The results of survival analysis showed that patients in the high-confidence group exhibited significantly higher overall survival ratio compared to the low-confidence group (Figure 7(e-f)). The p-values were 0.0038 and 0.031 for two cohorts, respectively. These findings suggest a strong association between the HLA- and TCR-peptide bindings predicted by UnifyImmun and favorable immunotherapy responses as well as clinical outcomes.

### 3 Discussion and Conclusion

In this study, we introduce UnifyImmun, a unified cross-attention-based model designed to simultaneously predict the binding specificity of antigens to both HLA and TCR molecules. We have devised a two-phase progressive training strategy by which the two tasks mutually reinforce each other, guiding the encoders to capture more distinctive features. To bolster the model’s generalizability, we have incorporated virtual adversarial perturbation into the framework. When benchmarked against over ten existing methods for antigen-HLA and antigen-TCR binding prediction, our method consistently outperforms them in both tasks on hold-out test set and external independent set, as well as HPV and COVID-19 test set. Additionally, the cross-attention scores pinpoint the amino acid sites crucial for antigen binding to receptors.

Most importantly, our model integrates the prediction tasks of antigen presentation and T-cell activation into a unified framework, offering more comprehensive evaluation of antigen immunogenicity compared to previous models that only considered individual tasks alone. However, it is important to note that the antigen-induced immune system activation involves a series of cascading biological process, with numerous factors influencing the immunogenicity of antigens. These include endopeptidase preferences for polypeptide cleavage sites, antigen concentration, stability of pHLA complexes, and transporter protein efficiency, all of which affect the degree of immune response activation. Although our model marks a significant advancement in the holistic assessment of antigen immunogenicity, it still represents a high-level simplification of the actual immune response process. This limitation could account for the suboptimal performance of our method on some test sets.

The currently available TCR CDR3 sequences constitute just a fraction of the immense human TCR repertoire. Despite our model could capture some antigen binding patterns from the TCR sequences, its capacity is hindered by the scarcity of available data. This constraint becomes particularly serious when confronted with unseen sequences in the test set, resulting in suboptimal prediction performance. Fortunately, Fortunately, the remarkable progress in single-cell transcriptome sequencing

has led to a significant increase in scRNA-seq data of T cells, greatly facilitating the acquisition of CDR3 sequences. By leveraging the power of large language models (LLM) for pre-training, we can extract more expressive and meaningful features from the wealth of sequences. This, in turn, has the potential to significantly enhance the predictive capabilities of our model, enabling it to more accurately assess the immunogenicity of antigens.

## 4 Methods

### 4.1 Dataset

We created a benchmark dataset of HLA-peptide bindings from over ten previous studies (for more details see Supplementary Table S1). After removing duplicates and abnormal sequences (such as missing values or asterisk), we obtained 423,843 pHLA binders, including 139 HLA alleles and 219,916 unique peptides. The dataset was subsequently split into the training set and hold-out test set by 9:1 ratio. As a result, the training set contained 381,287 pairs, spanning 139 HLA alleles and 219,916 antigens. The test set contained 42,556 pairs, covering 124 HLA alleles and 34,052 antigens.

Since previous studies have verified that both  $\alpha$  and  $\beta$  chains of TCR are crucial for antigen recognition [25, 54], we considered both chains and treated them as single CDR3 chains. This approach differed from existing models that only considered the  $\beta$  chain. Consequently, we created a TCR-peptide binding dataset with 109,554 pairs, which was split into training and hold-out test set by 9:1 ratio. The training set covered 881 distinct antigens and 93,727 unique CDR3 sequences, while the test set covered 496 distinct antigens and 10,896 unique CDR3 sequences. In addition, we built an independent test set composed of HLA-antigen-TCR triplet, which included 63,324 pairs covering 57 HLA alleles, 998 distinct antigens, and 53,439 CDR3 sequences.

To our best knowledge, both the HLA-antigen and TCR-antigen binding datasets we built are the largest to date. We shuffled the HLA (TCR) and peptide sequences, and randomly mismatched them to generate negative samples. Although false negative samples may be generated, the possibility and proportion of such samples are very low and can be ignored. We generated the same number of negative samples to positive samples to obtain balanced datasets.

### 4.2 Sequence embedding

The HLA pseudo sequences have a fixed length of 34 amino acids. Each amino acid is mapped to a 64-dimensional embedding via a character embedding layer. Since the order of amino acids is critical to the protein structure and function, the sine and cosine positional encoding is applied to each position. The amino-acid embedding and positional embedding are summed to obtain the sequence embedding.

The peptides are padded to maximum length of 15 to handle the variable input length, and then each amino acid is mapped to a 64-dimensional embedding. Similarly, the positional encoding is executed to incorporate positional information of the

amino acids. After the padding and embedding steps, each peptide is represented as a embedding matrix.

All the TCR CDR3 sequences shorter than 34 amino acids are padded to 34, while a small number of CDR3 sequences exceeding 34 amino acids are truncated. Next, the similar embedding process is applied to each CDR3 sequence.

### 4.3 Transformer-based encoder

The encoder is based on self-attention mechanism [55], which has shown exceptional capability in extracting global correlation and dependency relationships from protein sequences [56–58]. Self-attention mechanism learns the attention of all possible amino acid pairs in the input sequence. The attention scores are computed from the normalized dot product of query vectors  $Q$  and key vectors  $K$  followed by a softmax operation. The self-attention layer output the weighted sum of the value vectors  $V$  by the attention scores. The operations of a self-attention layer written in matrix form are as follows:

$$\text{Attention}(Q, K, V) = \text{softmax} \left( \frac{QK^T}{\sqrt{d_k}} \right) V \quad (1)$$

where  $d_k$  is the dimension of the vectors (chosen as 64). Taking HLA as an example, the  $Q$ ,  $K$ ,  $V$  are all set to its  $34 \times 64$  embedding matrix. Subsequently, the output of the self-attention block is passed through multiple fully-connected layers, by which the dimension of the gyro first rises and then falls. For peptides and TCR sequences, we adopt the similar encoder architecture for feature extraction.

It is important to highlight that we introduce the mask mechanism in calculating the self-attention scores. Specifically, for peptides or CDR3 sequences shorter than their respective maximum lengths, we exclude non-amino-acid characters from consideration during model training. For this purpose, we assign zero attention scores corresponding to these characters, so that they do not influence the computation of attention scores. In our implementation, the encoder comprises a one-layer one-head self-attention block.

### 4.4 Cross-attention for feature fusion

Cross-attention mechanism can effectively capture the intricate relationships and dependencies between different sequences [59, 60]. In our work, we leverage the cross-attention mechanism to extract crucial information regarding the interactions between peptide and HLA/TCR molecules. For the integration of HLA and peptide feature, the HLA embedding act as the  $K$  and  $V$  matrices, while the peptide embedding serves as the  $Q$  matrix. Subsequently, the  $V$  matrix is weighted based on the computed cross-attention scores between  $Q$  and  $K$ . The cross-attention layer’s output passes through three fully-connected layers: first expanding to 512 dimensions and then compressing to 64 for a condensed representation. The similar process is applied for the fusion of TCR and peptide features, where TCR embedding act as  $K$  and  $V$  matrices, and peptide embedding server as  $Q$  matrix.

We also employ mask mechanism in calculating the cross-attention scores. The mask mechanism greatly reduces the computational overhead and accelerates the

model’s convergence rate. In our implementation, we use one-head and one-layer cross-attention mechanism, as illustrated in Figure 1.

#### 4.5 Prediction of binding specificity

To predict the bindings between peptides and HLA (or TCR) molecules, we flatten the fused matrix of HLA (or TCR)-peptide pairs outputted by the cross-attention block, resulting in a 2176-dimensional vector (aka  $34 \times 64$ ). This vector then passes through three fully-connected layers with 256, 64, and 2 nodes, respectively, utilizing the ReLU activation function. The final output is obtained via a Softmax layer. We adopt cross-entropy as the loss function, and use the Adam optimizer with a learning rate of  $1e-3$ .

The model training is conducted on a CentOS Linux 8.2.2004 (Core) system, equipped with an Intel(R) Xeon(R) Silver 4210R CPU operating at 2.40GHz, along with a GeForce RTX 4090 GPU and 128GB of memory. The model is implemented using PyTorch 2.2.1.

#### 4.6 Virtual adversarial training

Virtual adversarial training [61] introduces subtle perturbations within the vicinity of the sequence embedding space, rather than directly perturbing the original sequences. The perturbations are oriented towards the direction of loss gradient ascent and are typically generated under L2 norm constraints. This training strategy demands that the model not only minimizes the original loss but also minimizes the adversarial loss, making the model less sensitive to slight changes in the input. We applied adversarial perturbations to the embeddings of all three types of sequences, so that the encoder learn to extract discriminative features. Our ablation experiments have confirmed that virtual adversarial learning indeed improves model performance, as shown in Table S1.

#### 4.7 Two-stage progressive training

In the first phase, the model was trained exclusively on the HLA-peptide pairs, keeping the TCR encoder and the TCR-antigen cross-attention module fixed. This enforced the model to concentrate solely on learning the intricacy of HLA-antigen interactions. In the second phase, the model were trained exclusively using the TCR-peptide pairs, with the HLA encoder and HLA-antigen cross-attention module fixed. These two phases were alternated until the model performance converged. Note that throughout the alternating training process, the antigen encoder remained continuously updated and shared between both HLA-antigen and TCR-antigen binding prediction tasks. By iteratively refining the antigen encoder parameters, the model learned to capture the essential information pertinent to both HLA and TCR binding and thereby enhanced its overall predictive accuracy.

#### 4.8 Model ablation experiments

To validate the contributions of different components, we conducted ablation studies on our model to assess the performance in predicting HLA-antigen and TCR-antigen

bindings. Specifically, we evaluate the attention masking, positional encoding, and virtual adversarial perturbation individually. The results obtained by the ablated models for antigen-HLA and antigen-TCR CDR3 binding are outlined in Table 1 and Table 2, respectively.

The findings reveal that the removal of any component leads to a decrease in performance when compared to UnifyImmun. Notably, the removal of virtual adversarial perturbation has the most significant impact, resulting in at least 4% drop in AUROC for both HLA-antigen and antigen-TCR binding predictions. This strongly indicates that virtual adversarial training contributes to improving the model’s overall performance and generalization capabilities. Furthermore, we observed that the absence of the attention masking leads to increased computational overhead during the training process. Without the mask, additional computational resources are expended to process padding sequences, leading to a rise in computational cost.

## References

- [1] Yang, K., Halima, A. & Chan, T. A. Antigen presentation in cancer—mechanisms and clinical implications for immunotherapy. *Nature Reviews Clinical Oncology* **20**, 604–623 (2023).
- [2] Barry, M. & Bleackley, R. C. Cytotoxic t lymphocytes: all roads lead to death. *Nature Reviews Immunology* **2**, 401–409 (2002).
- [3] Raskov, H., Orhan, A., Christensen, J. P. & Gögenur, I. Cytotoxic cd8+ t cells in cancer and cancer immunotherapy. *British journal of cancer* **124**, 359–367 (2021).
- [4] Weigelin, B. *et al.* Cytotoxic t cells are able to efficiently eliminate cancer cells by additive cytotoxicity. *Nature communications* **12**, 5217 (2021).
- [5] Rowen, L., Koop, B. F. & Hood, L. The complete 685-kilobase dna sequence of the human  $\beta$  t cell receptor locus. *Science* **272**, 1755–1762 (1996).
- [6] Glanville, J. *et al.* Identifying specificity groups in the t cell receptor repertoire. *Nature* **547**, 94–98 (2017).
- [7] Fowell, D. J. & Kim, M. The spatio-temporal control of effector t cell migration. *Nature Reviews Immunology* **21**, 582–596 (2021).
- [8] Lim, A. R., Rathmell, W. K. & Rathmell, J. C. The tumor microenvironment as a metabolic barrier to effector t cells and immunotherapy. *Elife* **9**, e55185 (2020).
- [9] Farber, D. L., Yudanin, N. A. & Restifo, N. P. Human memory t cells: generation, compartmentalization and homeostasis. *Nature Reviews Immunology* **14**, 24–35 (2014).



- [10] Liu, Q., Sun, Z. & Chen, L. Memory t cells: strategies for optimizing tumor immunotherapy. *Protein & cell* **11**, 549–564 (2020).
- [11] Chen, D. S. & Mellman, I. Oncology meets immunology: the cancer-immunity cycle. *immunity* **39**, 1–10 (2013).
- [12] Yewdell, J. W. & Bennink, J. R. Immunodominance in major histocompatibility complex class i-restricted t lymphocyte responses. *Annual review of immunology* **17**, 51–88 (1999).
- [13] Dunn, G. P., Old, L. J. & Schreiber, R. D. The three es of cancer immunoediting. *Annu. Rev. Immunol.* **22**, 329–360 (2004).
- [14] Trowsdale, J. Hla genomics in the third millennium. *Current opinion in Immunology* **17**, 498–504 (2005).
- [15] Huppa, J. B. *et al.* Tcr-peptide-mhc interactions in situ show accelerated kinetics and increased affinity. *Nature* **463**, 963–967 (2010).
- [16] Nikolich-Zugich, J., Slifka, M. K. & Messaoudi, I. The many important facets of t-cell repertoire diversity. *Nature Reviews Immunology* **4**, 123–132 (2004).
- [17] Zhang, S.-Q. *et al.* Direct measurement of t cell receptor affinity and sequence from naïve antiviral t cells. *Science translational medicine* **8**, 341ra77–341ra77 (2016).
- [18] Davis, M. M. & Bjorkman, P. J. T-cell antigen receptor genes and t-cell recognition. *Nature* **334**, 395–402 (1988).
- [19] Krogsgaard, M. & Davis, M. M. How t cells’ see’antigen. *Nature immunology* **6**, 239–245 (2005).
- [20] Chowell, D. *et al.* Evolutionary divergence of hla class i genotype impacts efficacy of cancer immunotherapy. *Nature medicine* **25**, 1715–1720 (2019).
- [21] Krishna, C., Chowell, D., Gönen, M., Elhanati, Y. & Chan, T. A. Genetic and environmental determinants of human tcr repertoire diversity. *Immunity & Ageing* **17**, 1–7 (2020).
- [22] Purcell, A. W., Ramarathinam, S. H. & Ternette, N. Mass spectrometry-based identification of mhc-bound peptides for immunopeptidomics. *Nature protocols* **14**, 1687–1707 (2019).
- [23] Zhang, S.-Q. *et al.* High-throughput determination of the antigen specificities of t cell receptors in single cells. *Nature biotechnology* **36**, 1156–1159 (2018).
- [24] Kula, T. *et al.* T-scan: a genome-wide method for the systematic discovery of t cell epitopes. *Cell* **178**, 1016–1028 (2019).

- [25] Hudson, D., Fernandes, R. A., Basham, M., Ogg, G. & Koohy, H. Can we predict t cell specificity with digital biology and machine learning? *Nature Reviews Immunology* **23**, 511–521 (2023).
- [26] Chu, Y. *et al.* A transformer-based model to predict peptide–hla class i binding and optimize mutated peptides for vaccine design. *Nature Machine Intelligence* **4**, 300–311 (2022).
- [27] O’Donnell, T., Rubinsteyn, A., Bonsack, M., Riemer, A. & Hammerbacher, J. Mhcflurry: open-source class i mhc binding affinity prediction. *Cold Spring Harbor Laboratory* (2017).
- [28] Birker, R., Bruno, A., Sinu, P., Bjoern, P. & Morten, N. Netmhcpa-4.1 and netmhciipa-4.0: improved predictions of mhc antigen presentation by concurrent motif deconvolution and integration of ms mhc eluted ligand data. *Nucleic Acids Research* .
- [29] Haoyang, Z. & Gifford, D. K. DeepLigand: accurate prediction of mhc class i ligands using peptide embedding. *Bioinformatics* i278–i283 (2019).
- [30] Jun, C., Kadre, B., Karola, R. & Brandon, M. Bertmhc: improved mhc–peptide class ii interaction prediction with transformer and multiple instance learning. *Bioinformatics* (2021).
- [31] Gao, Y. *et al.* Pan-peptide meta learning for t-cell receptor–antigen binding recognition. *Nature Machine Intelligence* **5**, 236–249 (2023).
- [32] Lu, T. *et al.* Deep learning-based prediction of the t cell receptor–antigen binding specificity. *Nature machine intelligence* **3**, 864–875 (2021).
- [33] Zhaochun, X. *et al.* Dlptcr: an ensemble deep learning framework for predicting immunogenic peptide recognized by t cell receptor. *Briefings in Bioinformatics* (2021).
- [34] Springer, I., Tickotsky, N. & Louzoun, Y. Contribution of t cell receptor alpha and beta cdr3, mhc typing, v and j genes to peptide binding prediction. *Frontiers in Immunology* **12**, 664514 (2021).
- [35] Weber, A., Born, J. & Martínez, M. R. Titan: T-cell receptor specificity prediction with bimodal attention networks. *Bioinformatics* **37**, i237–i244 (2021).
- [36] Fang, Y., Liu, X. & Liu, H. Attention-aware contrastive learning for predicting t cell receptor–antigen binding specificity. *Briefings in Bioinformatics* **23**, bbac378 (2022).
- [37] Massimo, A. & Morten, N. Gapped sequence alignment using artificial neural networks: application to the mhc class i system. *Bioinformatics* 511.

- [38] Zhang, H., Lund, O. & Nielsen, M. The pickpocket method for predicting binding specificities for receptors based on receptor pocket similarities. *Bioinformatics* (2009).
- [39] Kim, Y., Sidney, J., Pinilla, C., Sette, A. & Peters, B. Derivation of an amino acid similarity matrix for peptide:mhc binding and its application as a bayesian prior. *BMC Bioinformatics* **10** (2009).
- [40] Peters, B. & Sette, A. Generating quantitative models describing the sequence specificity of biological processes with the stabilized matrix method. *BMC Bioinformatics* **6**, 132 – 132 (2005).
- [41] Karosiene, E., Lundegaard, C., Lund, O. & Nielsen, M. Netmhcons: a consensus method for the major histocompatibility complex class i predictions. *Immunogenetics* **64**, 177–186 (2012).
- [42] Rasmussen *et al.* Pan-specific prediction of peptide-mhc class i complex stability, a correlate of t cell immunogenicity. *Journal of Immunology* (2016).
- [43] Moutaftsi, M. *et al.* A consensus epitope prediction approach identifies the breadth of murine t(cd8+)-cell responses to vaccinia virus. *Nature Publishing Group* (2006).
- [44] Yan, H. *et al.* Acme: pan-specific peptide–mhc class i binding prediction through attention-based deep neural networks. *Bioinformatics* **23**.
- [45] Jin, J. *et al.* Deep learning pan-specific model for interpretable mhc-i peptide binding prediction with improved attention mechanism. *Proteins* **89**, 866–883 (2021).
- [46] Vita, R. *et al.* The immune epitope database (iedb): 2018 update. *Nucleic acids research* **47**, D339–D343 (2019).
- [47] Bonsack, M. *et al.* Performance evaluation of mhc class-i binding prediction tools based on an experimentally validated mhc–peptide binding data set. *Cancer immunology research* **7**, 719–736 (2019).
- [48] Wells, D. K. *et al.* Key parameters of tumor epitope immunogenicity revealed through a consortium approach improve neoantigen prediction. *Cell* **183**, 818–834 (2020).
- [49] Wang, G. *et al.* Ineo-epp: a novel t-cell hla class-i immunogenicity or neoantigenic epitope prediction method based on sequence-related amino acid features. *BioMed research international* **2020** (2020).
- [50] Parker, K. C. *et al.* Sequence motifs important for peptide binding to the human mhc class i molecule, hla-a2. *Journal of immunology (Baltimore, Md.: 1950)* **149**,

3580–3587 (1992).

- [51] Van Allen, E. M. *et al.* Genomic correlates of response to ctla-4 blockade in metastatic melanoma. *Science* **350**, 207–211 (2015).
- [52] Alexandra, S. *et al.* Contribution of systemic and somatic factors to clinical response and resistance to pd-1l blockade in urothelial cancer: An exploratory multi-omic analysis. *PLOS Medicine* **14** (2017).
- [53] Tumor and microenvironment evolution during immunotherapy with nivolumab. *Cell* **171**, 934–949.e16 (2017).
- [54] Zhao, X. *et al.* Tuning t cell receptor sensitivity through catch bond engineering. *Science* **376**, eabl5282 (2022).
- [55] Vaswani, A. *et al.* Guyon, I. *et al.* (eds) *Attention is all you need*. (eds Guyon, I. *et al.*) *Advances in Neural Information Processing Systems*, Vol. 30 (Curran Associates, Inc., 2017).
- [56] Madani, A. *et al.* Large language models generate functional protein sequences across diverse families. *Nature Biotechnology* **41**, 1099–1106 (2023).
- [57] Brandes, N., Ofer, D., Peleg, Y., Rappoport, N. & Linial, M. Proteinbert: a universal deep-learning model of protein sequence and function. *Bioinformatics* **38**, 2102–2110 (2022).
- [58] Rives, A. *et al.* Biological structure and function emerge from scaling unsupervised learning to 250 million protein sequences. *Proceedings of the National Academy of Sciences* **118**, e2016239118 (2021).
- [59] Honda, S., Koyama, K. & Kotaro, K. *Cross attentive antibody-antigen interaction prediction with multi-task learning* (2020).
- [60] Dens, C., Laukens, K., Meysman, P. & Bittremieux, W. A cross-attention transformer encoder for paired sequence data. *bioRxiv* 2023–12 (2023).
- [61] Miyato, T., Dai, A. M. & Goodfellow, I. *Adversarial training methods for semi-supervised text classification* (2017).

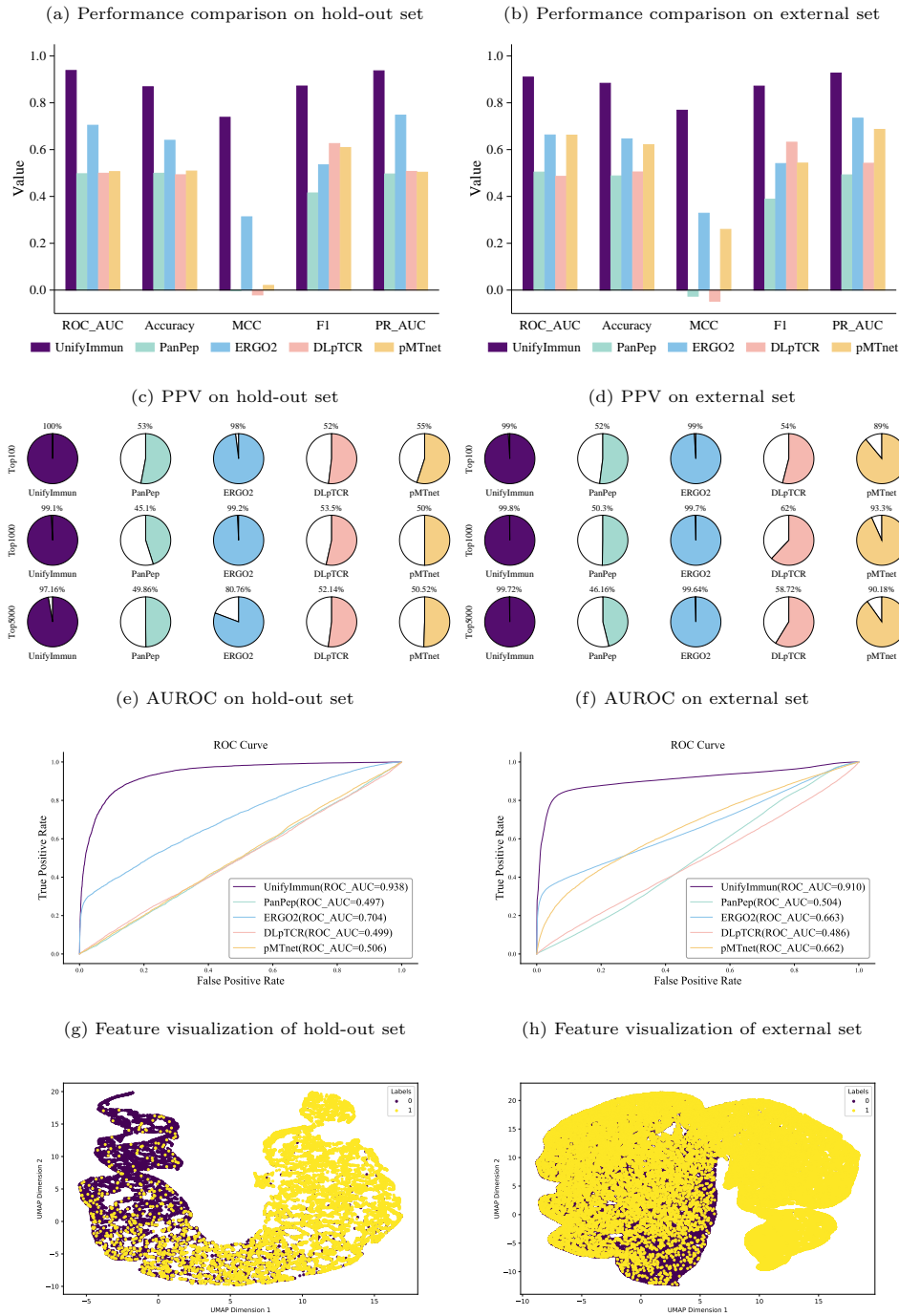


**Fig. 3:** Performance evaluation on predicting peptide-TCR binding specificity. (a-b) Performance comparison to four methods on hold-out and external test dataset, respectively. (c-d) Positive predictive value (PPV) for the top 100, top 1000, and top 5000 predicted samples on hold-out and external test dataset, respectively. (e-f) ROC curves and AUC values on hold-out and external test dataset, respectively. (g-h) UMAP feature visualization of peptide-CDR3 pairs.

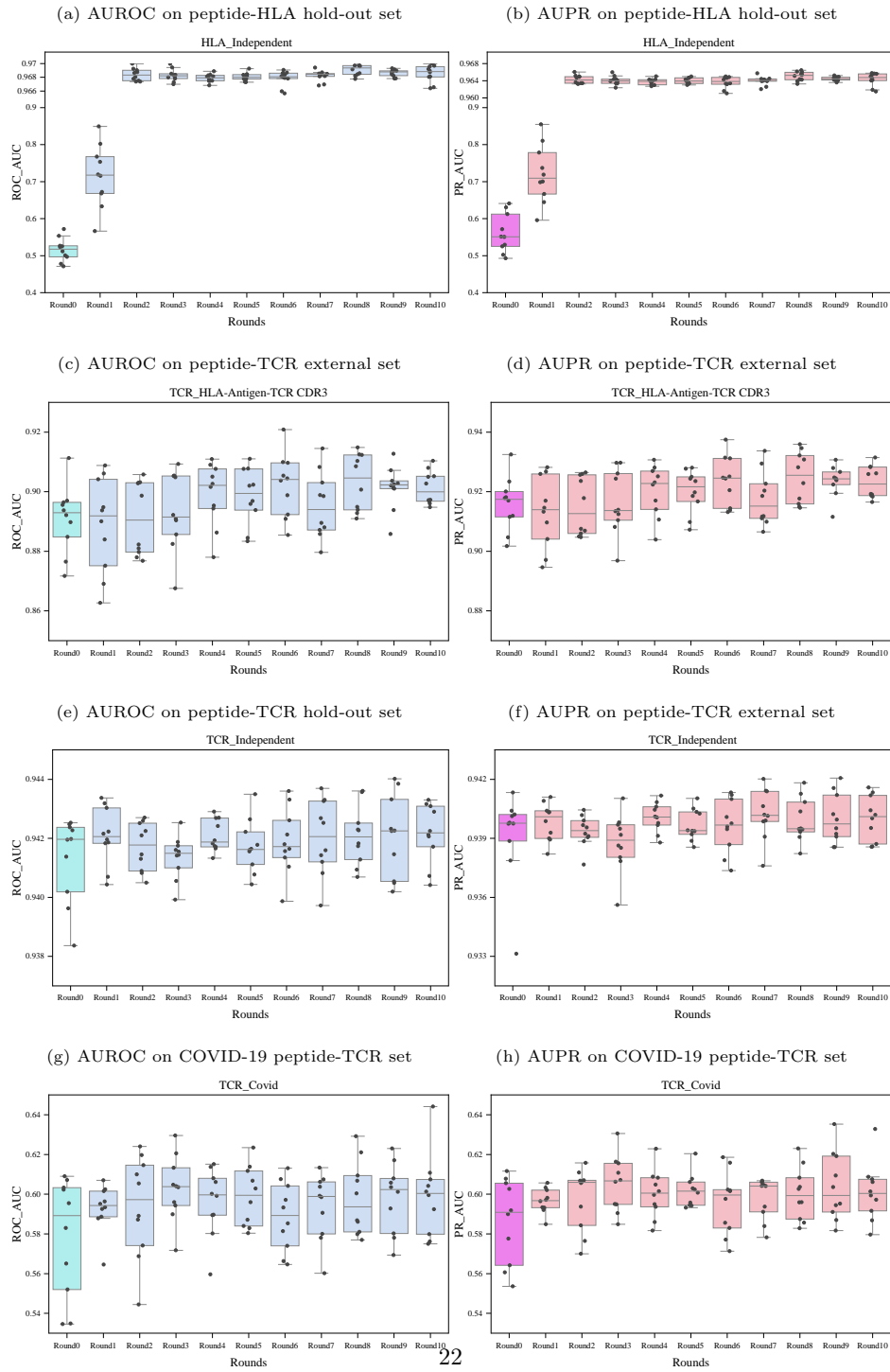
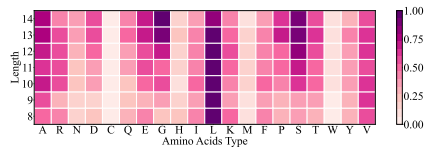
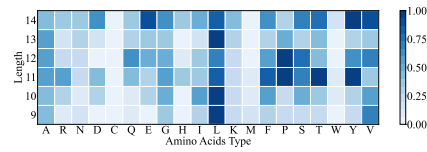


**Fig. 4:** Two-phase progressive training improved performance for both peptide-HLA and peptide-TCR binding prediction tasks. (a-b) AUROC and AUPR values increased with two-phase training rounds on peptide-HLA hold-out test set. (c-d) AUROC and AUPR values increased with two-phase training rounds on peptide-TCR external independent test set. (e-f) AUROC and AUPR values increased with two-phase training rounds on peptide-TCR hold-out test set. (g-h) AUROC and AUPR values increased with two-phase training rounds on peptide-TCR COVID-19 test set.

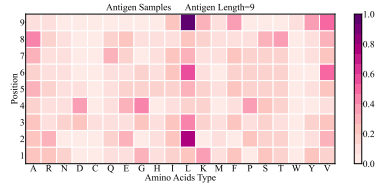
(a) Accumulative Attention scores for HLA binding



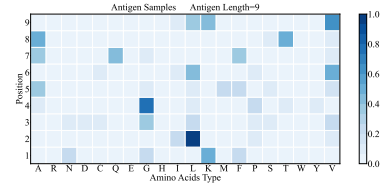
(b) Accumulative Attention scores for TCR binding



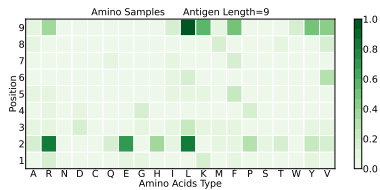
(c) Attention score for HLA binding



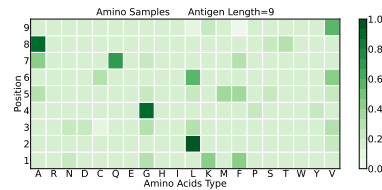
(d) Attention score for TCR binding



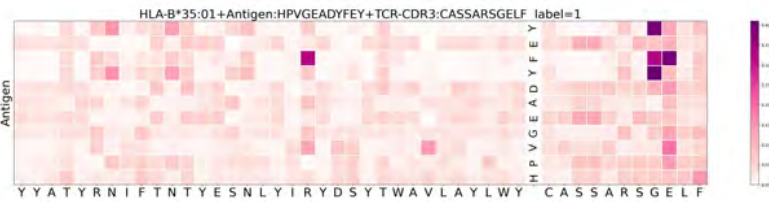
(e) Integral gradient for HLA binding



(f) Integral gradient for TCR binding



(g) Attention score-based heatmap for 3MV7 complex



(h) 3D structure for 3MV7 complex

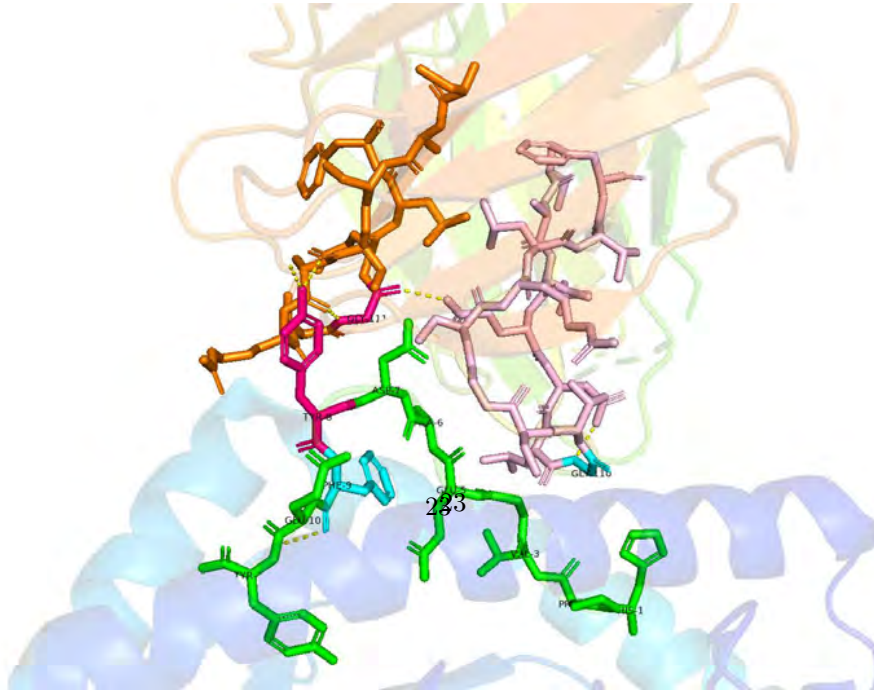


**Fig. 5:** Heatmaps based on cross-attention scores and integral gradients. (a-b) Accumulative contribution (attention score sum across peptide length) of each amino-acid type of peptide to pHLA and pTCR bindings, respectively. (c-d) Attention score-based heatmaps of the amino-acid type at each position of 9-mer peptide to pHLA and pTCR bindings, respectively. (e-f) Integral gradient-based heatmaps of the amino-acid type at each position of 9-mer peptide to pHLA and pTCR bindings, respectively. (g-h) Attention score-based heatmap and 3D structure for TCR complex with HLA-B\*35:01/HPVG (PDB ID: 3MV7).

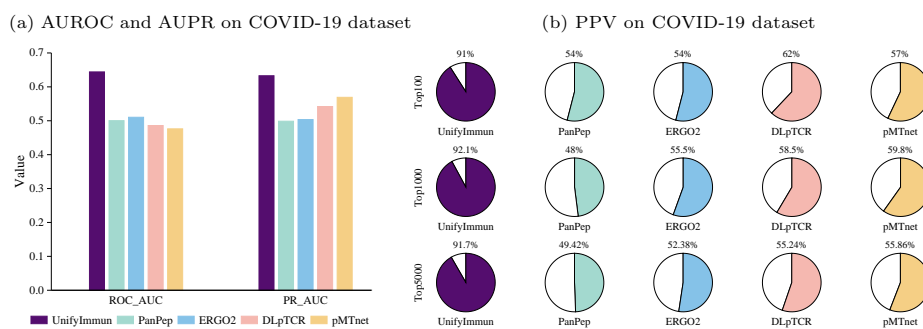


**Fig. 6:** Performance comparison to four existing methods on COVID-19 antigen-TCR CDR3 binding data set. (a) AUROC and AUPR values on COVID-19 dataset. (b) PPV of top100, top1000 and top5000 predicted samples on COVID-19 dataset.



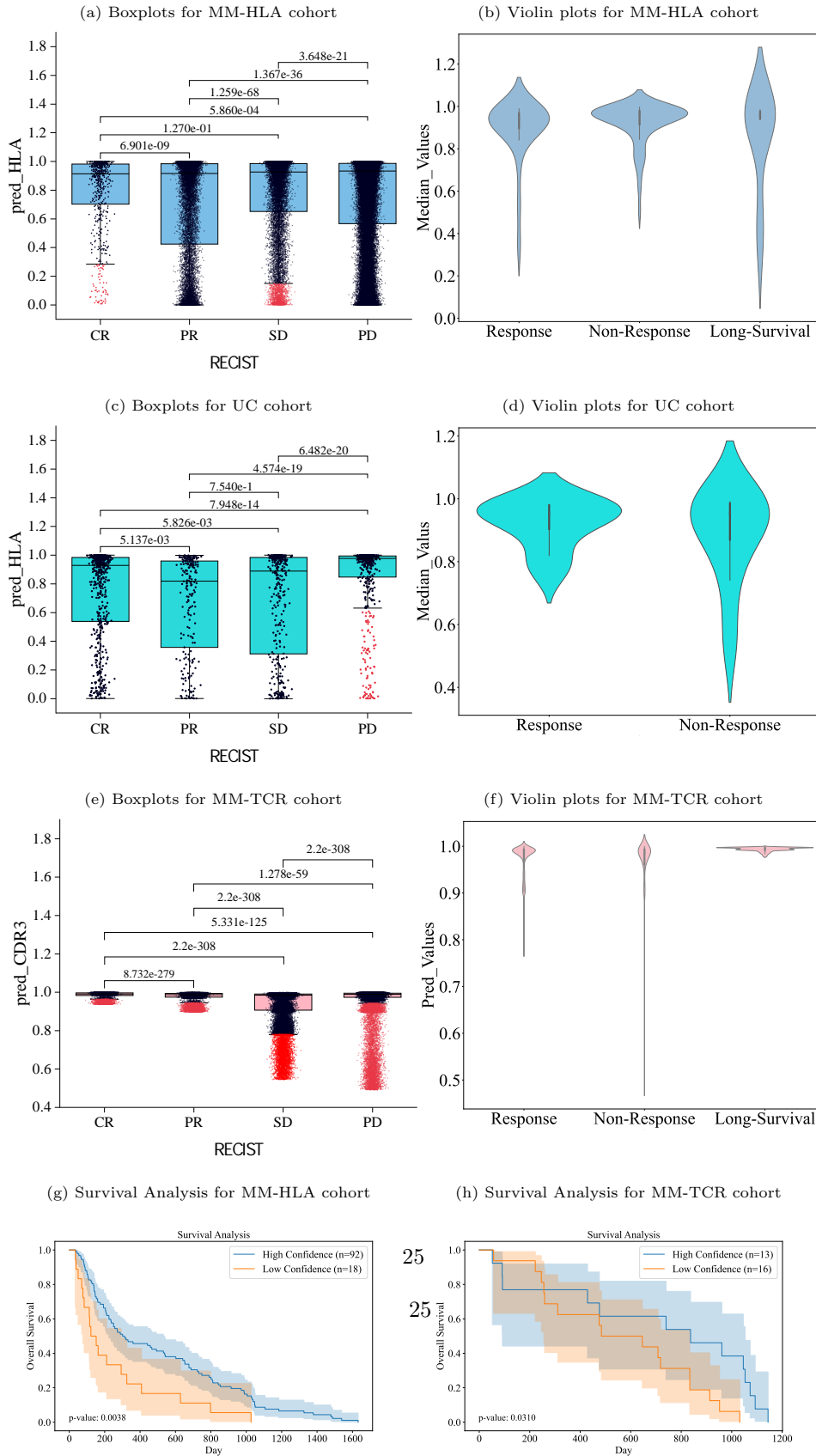


**Fig. 7:** Correlation between UnifyImmun predicted binding scores and immunotherapy response and clinical outcomes on three cohorts. (a-b) Boxplots and violin plots of predicted neoantigen-HLA binding scores regarding the different immunotherapy response groups for MM-HLA cohort, respectively. (c-d) Boxplots and violin plots of predicted neoantigen-HLA binding scores regarding the different immunotherapy response groups for UC cohort, respectively. (e-f) Boxplots and violin plots of predicted antigen-TCR binding scores regarding the different immunotherapy response groups for MM-TCR cohort, respectively. (g-h) Survival curves between stratified patient groups with high- and low-confidence antigen binding specificity on MM-HLA and MM-TCR cohorts.